IEEE Access
Multidisciplinary ⋮ Rapid Review ⋮ Open Access Journal

Received 1 October 2024, accepted 30 October 2024, date of publication 7 November 2024, date of current version 22 November 2024.

Digital Object Identifier 10.1109/ACCESS.2024.3493385

RESEARCH ARTICLE

mmWave Flat Panel Phased Array Antenna Module With Enhanced Scanning Coverage

YE-BON KIM[1], JONG-SIK MIN[2], SEONG-MO MOON[3], AND HAN LIM LEE[1,2], (Member, IEEE)

[1]School of Electrical and Electronics Engineering, Chung-Ang University, Seoul 06974, South Korea
[2]Department of Intelligent Semiconductor Engineering, Chung-Ang University, Seoul 06974, South Korea
[3]Satellite Payload Research Section, ETRI, Daejeon 34129, South Korea

Corresponding author: Han Lim Lee (hanlimlee@cau.ac.kr)

This work was supported in part by the Development of Civil Military Technology Project from the Institute of Civil Military Technology Cooperation (ICMTC) under Grant 21-CM-RA-02; and in part by the Institute for Information & communications Technology Planning & Evaluation (IITP) grant funded by the Korea Government (MSIP) (No. 2018-0-00190, Development of Core Technology for Satellite Payload)

ABSTRACT A compact mmWave phased array antenna module (PAAM) with wide beamwidth radiators to ensure seamless mmWave communication is proposed in this article. Unlike the typical PAAM consisting of patch-type elements with limited half power beamwidth (HPBW) around 90°, the proposed PAAM is configured by balanced multipole elements with extended HPBW in both E- and H-planes. Due to the extended HPBW of the proposed antenna element, the proposed PAMM can steer main beams for wider angles with lower side lobe levels. First, a single mmWave wide HPBW antenna element was fabricated and verified at 28 GHz, showing the measured HPBW of 148.3° and 141.3° in E- and H- planes, respectively. The measured HPBW of the proposed antenna showed more than 96% inrease in both planes, comparing with the conventional patch at 28 GHz. Moreover, 1 × 4 PAAM was fabricated by integrating the antenna array directly with a 4-channel beamforming IC to further verify the mmWave communications at 28 GHz with minimized blind spots. With 64-QAM over-the-air (OTA) test, the proposed PAAM showed the measured error vector magnitude (EVM) less than 7.1% at ±75° ranges while the conventional patch-based PAAM showed the measured EVM of 27.8% at ±75°.

INDEX TERMS mmWave antenna, phased array antenna module, wide angle scanning array, wide beamwidth antenna.

I. INTRODUCTION

With the evolution of industrial technology, the demand for innovative solutions to enhance efficiency, productivity, sustainability, and safety of machines keeps increasing more than ever. In particular, the adoption of autonomous robots into industrial sites can efficiently increase both efficiency and productivity with high flexibility at work. Thus, connected autonomous robots are considered as a key technology in the next generation smart industrial environments [1], [2], [3]. Under fully connected autonomous conditions, low-latency communications must be guaranteed for successful and safe operations because large number of autonomous robots must interact each other while recognizing the surrounding conditions. At the same time, since the industrial applications require large volume of data collected and shared with massive number of sensors, and processed by controllers, high data rate must be supported to enable real-time operations. Therefore, the use of mmWave spectrum becomes inevitable and the deployment of mmWave private-5G (P5G) network is rapidly attracting wide attention in both industry and industrial internet of things (IIoT) applications [4], [5], [6].

Fig. 1 describes the exemplar operations of connected autonomous robots under mmWave P5G networks. The robots must operate with real-time communications while integrating all data from connected robots and any IIoT

The associate editor coordinating the review of this manuscript and approving it for publication was Photos Vryonides.

© 2024 The Authors. This work is licensed under a Creative Commons Attribution-NonCommercial-NoDerivatives 4.0 License.
For more information, see https://creativecommons.org/licenses/by-nc-nd/4.0/

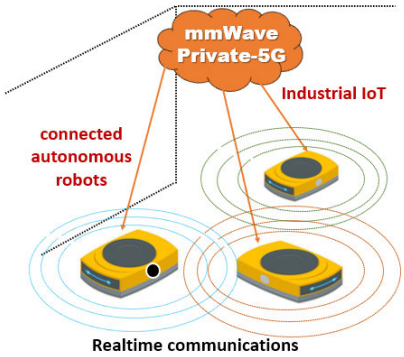


FIGURE 1. Connected autonomous robot with real-time operation by mmWave private-5G networks.

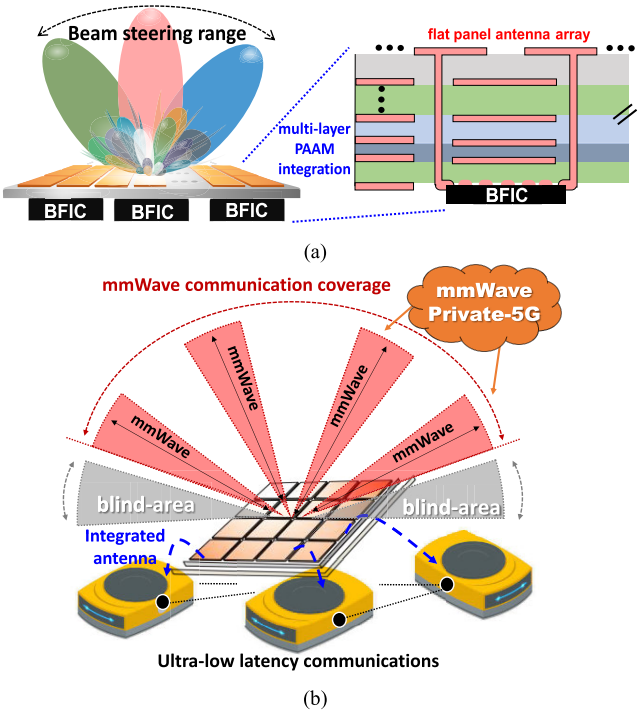


FIGURE 2. Phased array antenna module: (a) description for planar geometry and integration with BFIC and (b) communication coverage and blind communication spot due to limited beam-steering range.

devices associated with their mobility and tasks. To establish reliable mmWave communications while overcoming the high propagation loss and limited coverage at mmWave, beamforming technique must be effectively used to maintain the mmWave-based connectivity. Furthermore, the mmWave antennas must be compactly integrated with the robots' metallic body or IIoT devices without performance degradation, and communication or sensing blind spots. Fig. 2 (a) describes the physical requirement of mmWave phased array antenna module (PAAM). To avoid antenna performance degradation due to robot body effect and unnecessary overhanging structure on the robot body, planar antenna types with hemispherical coverage are required. Also, the planar antenna structures are necessary to efficiently integrate the array with beamforming integrated circuits (BFIC) through the typical multilayer printed circuit board (PCB) process [7], [8], [9], [10]. Although PAAM can steer the direction of main beams by shifting element phases, the scanning range of PAAM is limited by the limited half power beamwidth (HPBW) of single antenna element [11], [12], [13], [14]. Consequently, the limited scanning range becomes the limited mmWave communication range as described in Fig. 2 (b). Since connected autonomous robots continuously move, even wider scanning range to retain ultra-low latency mmWave communication must be ensured. In order to achieve wide beam steering characteristics in the mmWave band, lens-type antennas have been mainly studied [15], [16], [17], [18], [19]. However, due to the large volume and height of the lens, the cost increases, making it inefficient to use in actual products. In contrast, magnetic dipole or shorting pin antennas, which are planar structures, have been studied to overcome the high-profile structure [20], [21], [22], [23]. However, these antennas require a large ground size to achieve wider beamwidth or beam steering characteristics while also suffering from a narrow impedance bandwidth and asymmetrically expanded beamwidth in the E- and H-planes.

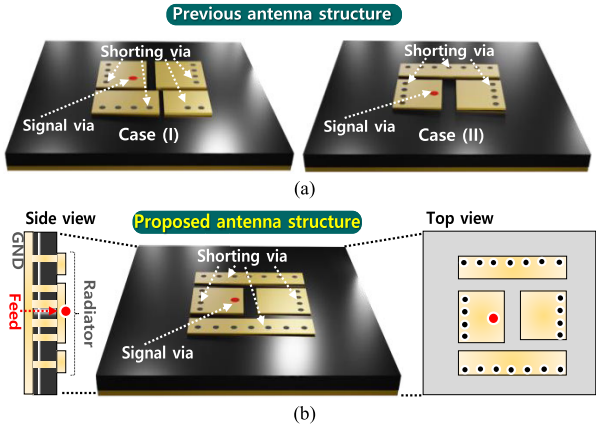


FIGURE 3. Multipole structures: (a) previously reported multipole antennas [24], [25] and (b) the proposed balanced multipole antenna.

To overcome these problems, multipole antennas, which have wide beamwidth and beam steering characteristics for both E- and H-planes, and a planar structure were previously reported [24], [25] as shown in Fig. 3 (a). However, the previous multipole antenna still showed an imbalance in the beamwidth expansion ratio for both E- and H-planes. Additionally, its unbalanced structure led to increased cross-polarization performance, presenting a challenge that requires further improvement. Thus, this paper proposes a new multipole antenna with a balanced structure, offering improved 2-D wide beam directionality and reduced cross-polarization characteristics compared to the previous models. Furthermore, this paper is the first to present and validate the multipole antenna structure in the mmWave band using actual modulation signals to affirm the blind-spotless communication coverage. That is, a compact

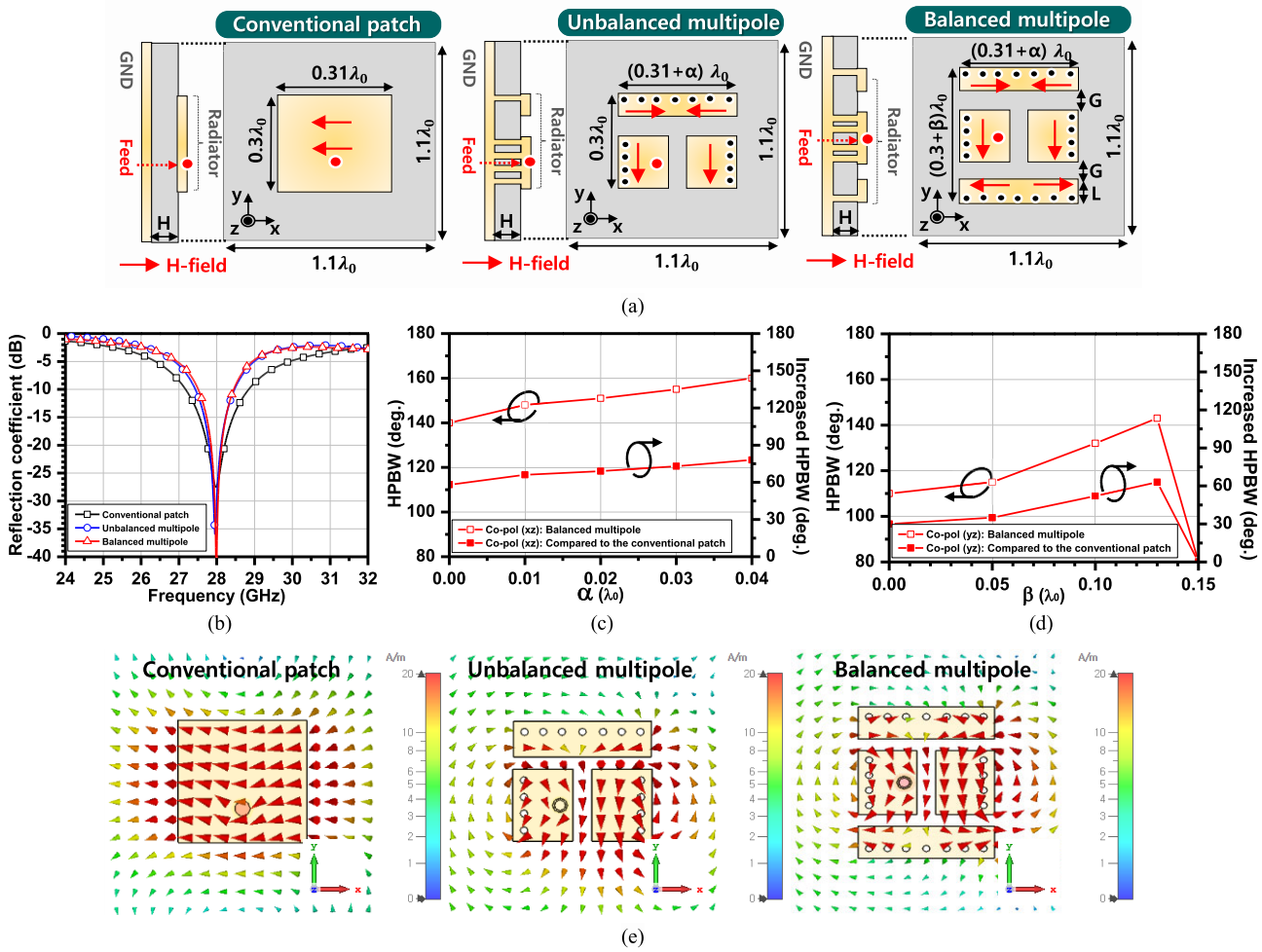


FIGURE 4. Conventional patch, previous and proposed multipole antenna with (a) configuration: The simulated (b) reflection coefficient, and HPBW and increased HPBW compared to the conventional patch antenna in xz and yz-planes at 28GHz with the effect of variation in (c) α and (d) β, and (e) H-field distribution.

mmWave PAAM, based on the balanced multipole antenna element, is verified for the n261 band to support mmWave P5G applications in this paper, as shown in Fig. 3 (b).

II. DESIGN AND ANAYSIS OF THE PROPOSED PAAM

A. ANALYSIS OF THE PROPOSED BALANCED MULTIPOLE ANTENNA

In this section, the proposed balanced multipole antenna is compared with the widely used planar patch antenna and previously reported unbalanced multipole antenna as shown in Fig. 4 (a). The single element patch antenna was first designed as a reference with a ground size of 1.1 $\lambda_0 \times 1.1\ \lambda_0$ at a center frequency of 28 GHz and a Taconic TLY-5 substrate thickness of 0.51 mm. The patch radiator size was 0.31 $\lambda_0 \times 0.3\ \lambda_0$ at 28 GHz. Then, the previously reported multipole antenna denoted as an unbalanced multipole was also designed at 28 GHz to demonstrate the novelty of the proposed antenna structure. It is noted that the previously reported antenna is defined as the unbalanced multipole structure in this article due to the asymmetrically positioned conductors. The fundamental principle of multipole antenna is the increase in antenna radiation aperture size by increasing the physical size of radiator while maintaining the resonance frequency through multiple electric and magnetic dipoles. By using multiple shorted conductors and spacing them, an increase in the capacitance value is induced, which is then compensated by additional inductance values through ground shorting vias, enabling impedance matching at the desired frequency band. However, in the case of the previously reported unbalanced multipole antennas [24], [25], it exhibited asymmetrically increased beamwidth in the E- and H-planes because the physical size of the radiator was extended toward only one direction compared to the conventional patch antenna. Therefore, the balanced multipole antenna structure, which achieves a wide beamwidth characteristic in both planes by extending the physical size of the radiator toward both planes, is proposed in this paper as shown in Fig. 4 (a). The proposed structure adopts the additional shorted conductor, making the radiator symmetric in E- and H-planes. Then, Fig. 4 (b) presents the

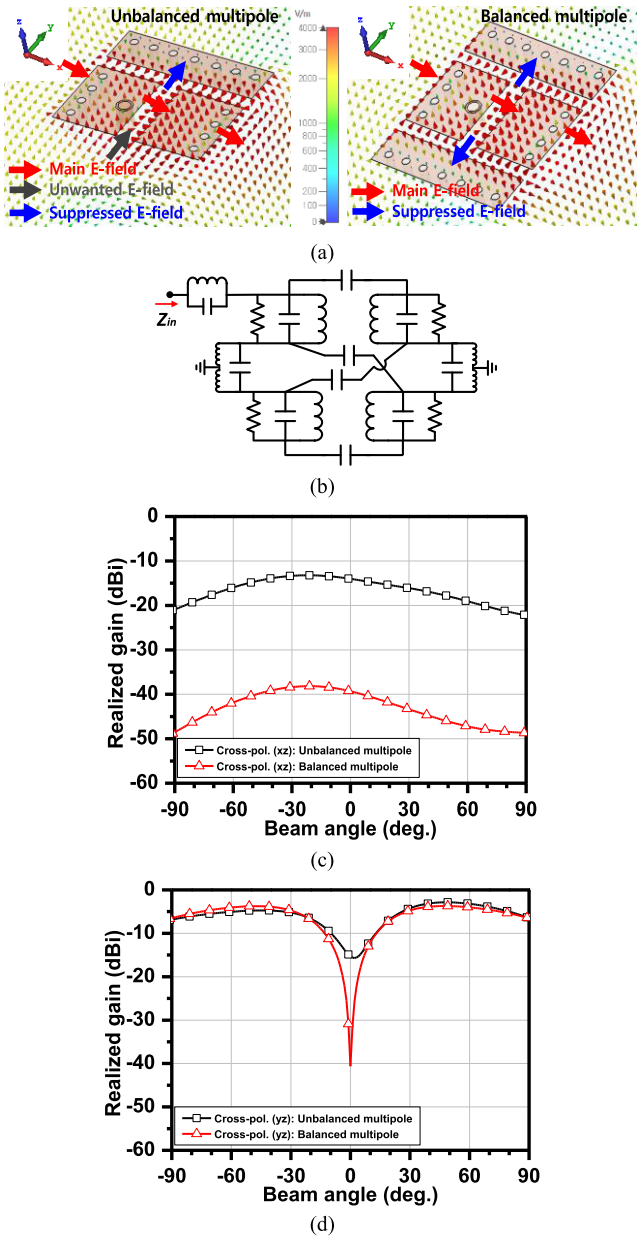


FIGURE 5. Simulated previous and proposed multipole antenna: (a) E-field distribution, (b) equivalent circuit of the proposed structure, and cross-polarization in (c) xz-plane and (d) yz-plane at 28 GHz.

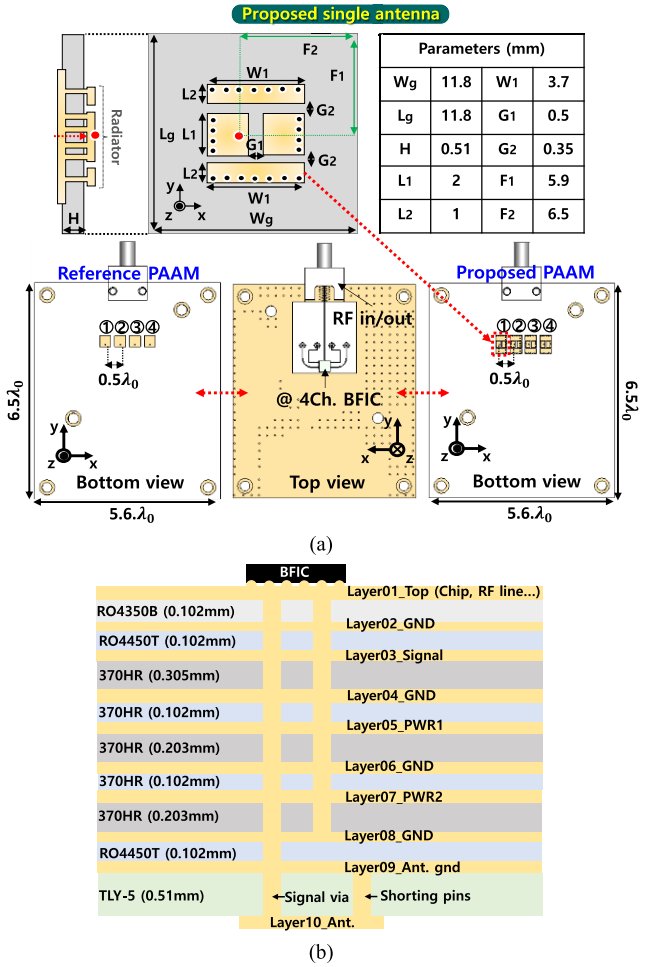


FIGURE 6. PAAM configuration with reference and proposed antenna of the (a) overview and (b) 1 × 4 antenna array and 4-ch beamforming IC layout structure overview.

simulation results of the reflection coefficient well-matched at the 28 GHz band for the conventional patch antenna, the previous unbalanced multipole antenna, and the newly proposed balanced multipole antenna. Furthermore, matching in the proposed multipole antenna can be achieved within the desired band by compensating for the increased capacitance value between the radiators and the ground shorting via inductance value. Next, Fig. 4 (c)-(d) analyze the extent to which wider beamwidth characteristics can be obtained compared to the patch antenna, with the increased radiation aperture size, designated as α and β, in both xz and yz-planes of the enlarged radiator. Fig. 4 (c) shows the simulation results of the increased beamwidth in the xz-plane for the proposed balanced multipole antenna compared to the conventional patch antenna. As the radiator from the conventional patch antenna increased from 0.31 λ_0 to 0.31 λ_0 + α in the xz-plane, the HPBW increased noticeably similar to the unbalanced multipole antenna. However, unlike the unbalanced structure, the proposed balanced multipole radiator was further enlarged in yz-plane to 0.3 λ_0 + β and showed the increased HPBW in both planes as depicted in Fig. 4 (d). However, when β exceeds 0.14 λ_0, a null appeared in the radiation pattern at the center angle in the yz-plane, reducing the beamwidth. Thus, considering both xz and yz- planes, α and and β are set to 0.03 λ_0 and 0.13 λ_0, respectively for the most effective beamwidth expansion. Therefore, the proposed single antenna could achieve the beamwidth characteristics of over 140° in all directions. Moreover, as shown in Fig. 4 (e), the H-field distributions of the conventional patch antenna, the unbalanced multipole antenna, and the proposed balanced multipole antenna were analyzed using a 3-D simulation tool. The proposed multipole antenna, having the widest aperture size, exhibits

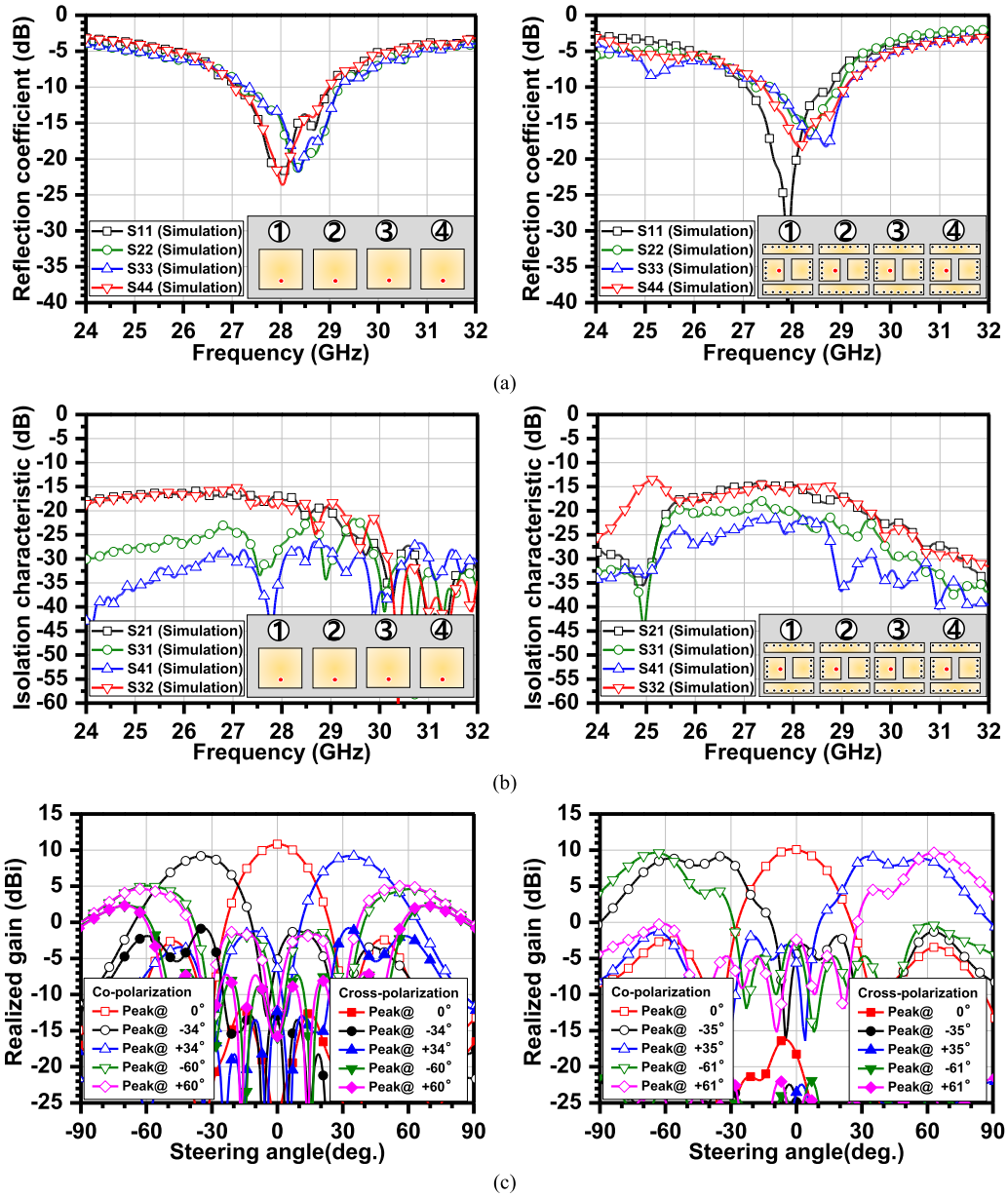


FIGURE 7. Simulated reference and proposed PAAM results for (a) reflection coefficient, (b) isolation characteristics and (c) beamforming characteristics at 28GHz.

a broader field distribution, thus demonstrating increased beamwidth characteristics in all directions. Subsequently, the cross-polarization performance of both the conventional and the proposed multipole antennas was analyzed. Since the conventional multipole antenna was designed to be unbalanced, it exhibited a slight increase in the cross-polarization phenomenon. However, this issue can be mitigated by adopting a balanced design for the multipole antenna as depicted in Fig. 5 (a) In the proposed balanced multipole antenna, the unwanted E-fields, introduced by the radiator's ground shorting via, can suppress the vertical component of the main E-field. Also, Fig. 5 (b) shows the equivalent RLC circuit model of the proposed structure. Since a trial-and-error-based curve-fitting process is required to extract the exact RLC values, only the equivalent circuit configuration is depicted in this paper. Then, Fig. 5 (c)-(d) presents the radiation pattern results for each antenna's pole at the 28 GHz band. When comparing the previous multipole antenna with the proposed antenna, the xz-plane showed a difference of more than 20 dBi at all angles. Additionally, an improvement in cross-polarization characteristics was confirmed within the proposed angles in the yz-plane.

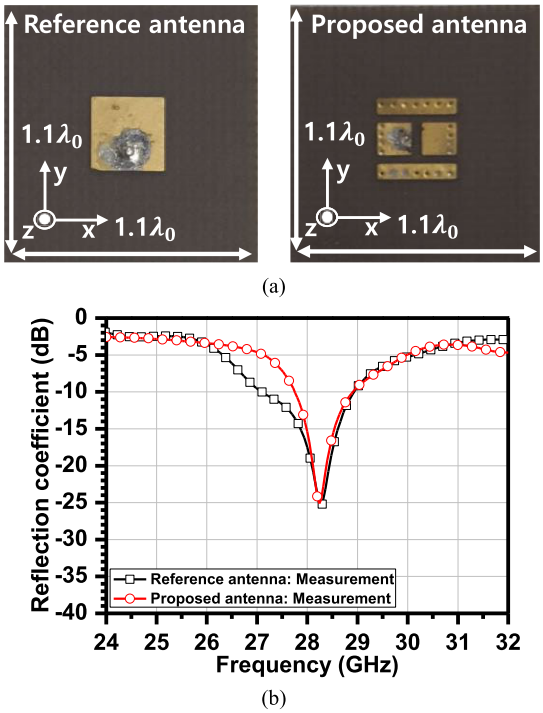


FIGURE 8. Proposed antenna element with (a) fabricated photos including the reference patch antenna, and (b) measured reflection coefficient.

B. DESIGN OF THE PROPOSED 1 × 4 ANTENNA ARRAY

Next, the performance of the finally designed single patch antenna and the proposed balanced multipole antenna with a 1 × 4 array antenna are compared as shown in Fig. 6 (a). Additionally, it also includes the design parameter values of a balanced single multipole antenna. To compare the performance of the antennas under the same conditions, the same array spacing (0.5 λ_0) and overall volume dimensions including the ground size (5.6 λ_0× 6.5 λ_0 × 0.16 λ_0) are specified as shown in Fig. 6 (a). Since a beamforming IC chip is required to steer the beam of the antenna, a modularized design was used to drive it. In addition, the overall layer-by-layer layout structure and board information are the same as shown in Fig 6 (b). To verify S-parameters and beamforming characteristics of the reference PAAM and proposed PAAM, a complete 1 × 4 antenna module is designed at 28 GHz as described in Fig. 7. Firstly, the reflection coefficients and isolation characteristic performances for antenna radiators within the array configuration are simulated as shown in Fig. 7 (a)-(c). Fig. 7 (a) shows the minimum 10-dB impedance bandwidths of 6.78% (27.1-29.0 GHz) and 6.07% (27.4-29.1 GHz) for the 1 × 4 reference PAAM and proposed PAAM respectively. Within the operational impedance bandwidth, the simulated isolation characteristics between antenna radiators for the 1 × 4 reference PAAM and proposed PAAM are better than −15 dB and −14 dB, respectively as shown in Fig. 8 (b). The radiation beam patterns are shifted with several arbitrary angles until the side lobe level (SLLs)

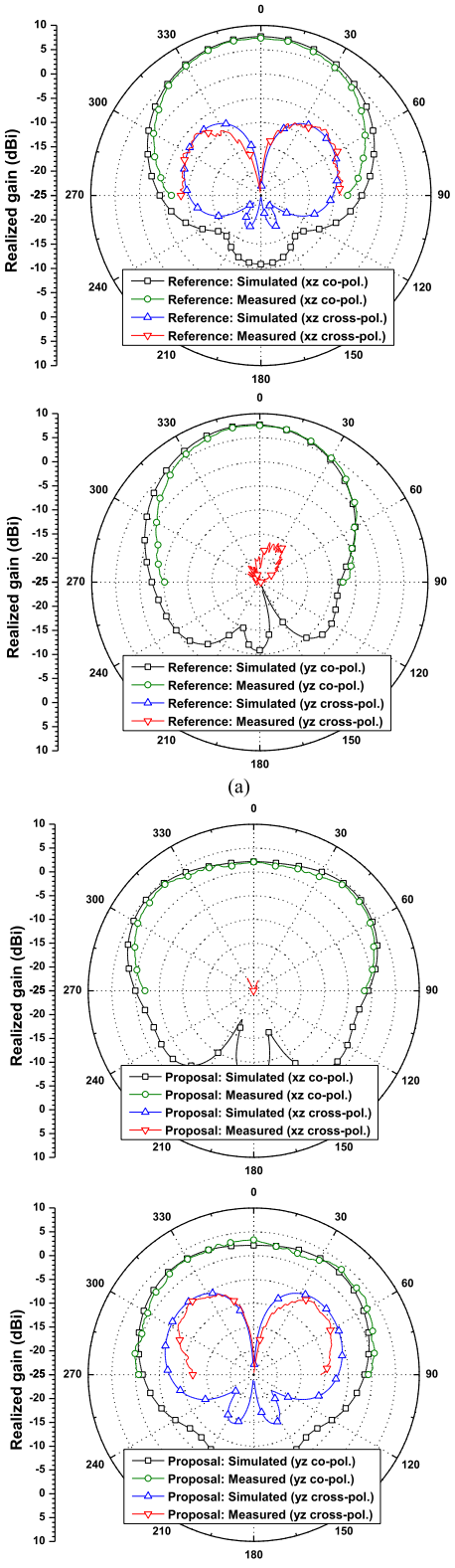


FIGURE 9. Measured radiation patterns of the reference patch and proposed antennas in both xz and yz planes: (a) reference patch and (b) proposed antennas.

exceeds −10 dB. The 3-dB beam-scanning angles with the SLLs of less than −10 dB for the reference PAAM and

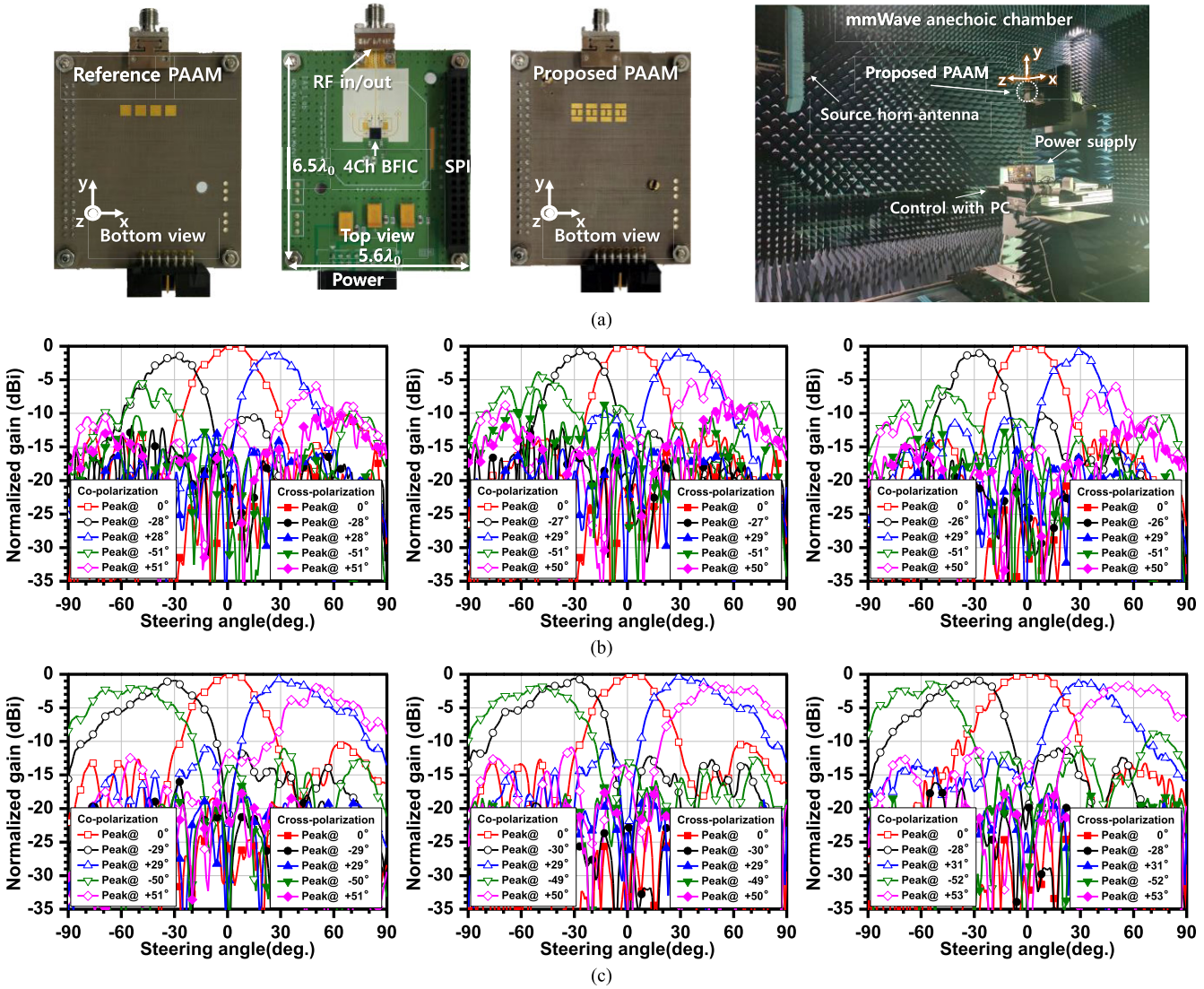


FIGURE 10. Measured beamforming patterns in xz-plane at 27.5, 28.0, 29.0 GHz for the (a) mmWave anechoic chamber setup (b) reference and (c) proposed PAAMs.

proposed PAAM are about 100° and 164°, respectively at 28 GHz as shown in Fig. 7 (c). In the case of a conventional PAAM, as the beam is steered, the SLL at opposite angles increase rapidly, and the cross-polarization characteristics increase. In addition, the center realized gain of the beam decreases rapidly. However, in the case of the proposed PAAM, the SLL and cross-polarization characteristics do not degrade as the beam is steered, and the gain decrease is very small. This is a result of the balanced structure design of the multipole antenna, which has a wide beamwidth and low cross-polarization characteristics from the single antenna characteristics.

III. FABRICATION AND MEASUREMENT

A. SINGLE ANTENNA ELEMENT MEASUREMENT

The proposed balanced multipole antenna was fabricated and compared with the conventional patch antenna at 28 GHz. To compare the typical patch antenna and the proposed antenna under the same conditions, a Taconic TLY-5 substrate was used, having a relative permittivity of 2.2, a loss tangent of 0.0009, and a thickness of 0.51 mm (0.047 λ0). The conducting layers were printed with 1/2 oz copper. Additionally, both antennas had the bottom layers as the ground planes, each with the same size of 11.8 mm × 11.8 mm (1.1 λ0 × 1.1 λ0), resulting in two-layer probe feeding printed circuit board (PCB) antennas, as shown in Fig. 8 (a).

Firstly, the measured 10 dB impedance bandwidths of reference antenna and proposed antenna were 6.42% (27.1-28.9 GHz) and 4.28% (27.7-28.9 GHz) as shown in Fig. 8 (b). Next, the Fig. 9 (a) shows the simulated and measured radiation patterns of the reference patch antenna at 28 GHz. The measured peak gains in both xz and yz- planes were about 7.7 dBi. Also, the measured HPBWs in the xz and yz- planes were 75.5° and 66.9°, respectively. Lastly, the

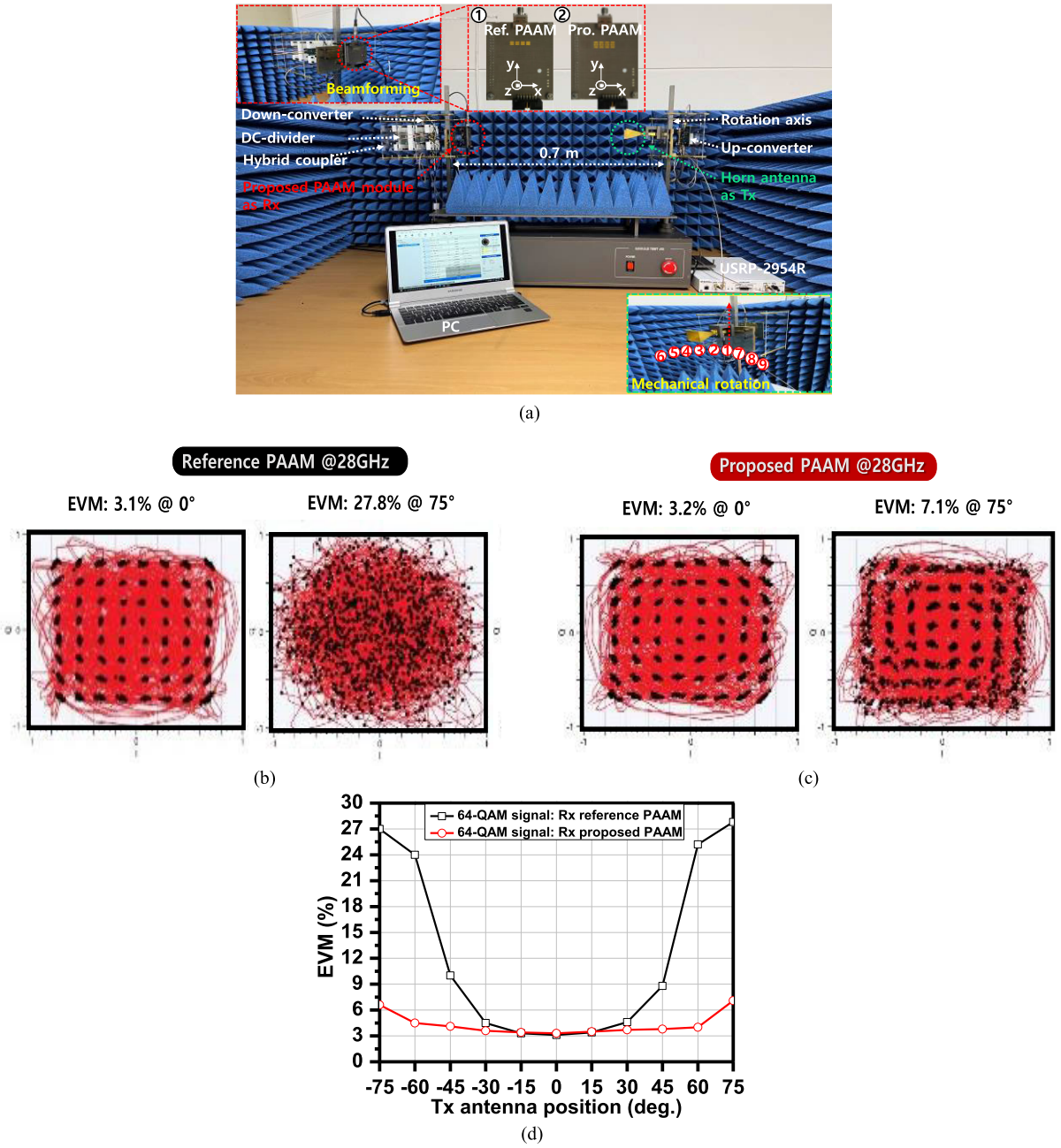


FIGURE 11. (a) 64-QAM signal OTA test environment, and measured EVM at 28GHz of the (b) reference PAAM, and (c) proposed PAAM, and (d) performed a comparison at arbitrary scan angles.

Fig. 9 (b) shows the simulated and measured radiation pattern of the proposed balanced multipole antenna at 28 GHz. The measured peak gains in both xz and yz- planes were about 5.2 dBi. Also, the measured HPBWs in xz and yz planes were 148.3° and 141.3°, respectively. Therefore, there were measured that the proposed balanced multipole antenna has a wide beamwidth characteristic in both planes, although the gain is somewhat reduced compared to the conventional patch antenna.

B. PROPOSED PAAM FABRICATION AND MEASUREMENT

The optimized typical patch antenna and the proposed balanced multipole antenna elements were extended to 1 × 4 array antennas and fabricated under the same antenna spacing (0.5 λ0) and total volume size (5.6 λ0 × 6.5 λ0 × 0.16 λ0) conditions for comparative analysis, as depicted in Fig. 10 (a). Also, a beamforming IC chip (Anokiwave 0162) was used to vary the magnitude and phase of each antenna element. This commercially available chip operates in the bandwidth

TABLE 1. Comparison of the proposed PAAM with other mmWave wide-angle scanning antennas.

Ref	Array size	Phase control	Antenna type	Center freq. (GHz)	10-dB IBW (%)	Peak gain (dBi)	HPBW steering angle (°)*	64-QAM EVM @ 75° (%)
[15]	1×8	Passive feed network	Dielectric lens	27.3	3.57	19	±70	N/A
[16]	14×18	PIN diodes	Rotman lens	24	16.6	12	±67	N/A
[17]	6×5	Passive feed network	Dielectric lens	28	7.14	21.2	±72	N/A
[18]	1×11	Passive feed network	Luneburg lens	29	35	15.4	±72	N/A
[19]	1×4	Passive feed network	Dielectric lens	28	7.14	20.3	±70	N/A
This work	1×4	BFIC	Flat panel	28	4.28	10	±78	7.1

* *Maintaining SLL lower than -10 dB*

of 26.5-29.5 GHz on a 4-channel. Both the reference and proposed PAAM were fabricated by modularizing each antenna, and the normalized gain beamforming characteristics were measured in the 27.5, 28.0, and 29.5 GHz bands in a mmWave anechoic chamber, as shown in Fig. 10 (a). The reference PAAM beam steering patterns were measured as shown in Fig. 10 (b). The beam patterns were steered at several arbitrary angles until the steering patterns were measured as showed in Fig. 10 (c). The 3-dB beam steering angles that satisfied SLLs lower than −10 dB were 158°, 156°, and 156°, respectively, at 27.5, 28, and 29.5 GHz. It was confirmed that the proposed PAAM has a wider beam steering characteristic compared to the reference PAAM, while maintaining low gain variation and low cross-polarization during beam steering.

Next, to verify the reference PAAM and proposed PAAM, over-the-air (OTA) EVM performance was tested with NR USRP-2954R 64-QAM signals. Fig. 11 (a) displays the measurement setup, where USRP-assisted baseband and IF, mmWave up-converters, and mmWave down-converter with a reference horn antenna were implemented. Fig. 11 (b)-(d) depicts the measured error vector magnitude (EVM) at 28 GHz with 64-QAM and different positions of Tx horn antenna beamforming reference and proposed PAAM performances. The Tx output power was -25.8 dBm without the commercialized horn antenna, and the Tx commercialized horn antenna gain was about 20 dBi at 28 GHz. The distance between the Tx and Rx antenna modules was 0.7m in the test setup. The worst measured EVMs of Rx proposed PAAM was 7.1%, whereas the reference PAAM was 27.8%. Hence, the proposed PAAM demonstrated excellent EVM measurement, better than the reference PAAM at all positions of Tx horn antenna.

Lastly, the proposed PAAM was compared with other state-of-the-art mmWave wide-angle scanning antennas, as summarized in Table 1. As shown in the comparison table, lens-type antennas have typically been used to achieve wide beam steering characteristics in the mmWave band. However, they are inefficient for use in real products due to their large size and increased fabrication complexity. Additionally, some structures require extra passive feed lines and PIN diode components, which cause high losses or additional power consumption in the mmWave applications. More importantly, the proposed PAAM demonstrates the widest beam steering angles compared to other architectures, despite its flat configuration. Furthermore, the proposed work is the only architecture verified through a 64-QAM OTA test, showing excellent EVM performance. Therefore, the proposed PAAM, with its small number of antennas, flat panel structure, wide beam steering characteristics, and low SLL and cross-polarization, can be a good candidate for connected autonomous robots and IIoT applications.

IV. CONCLUSION

In this paper, a novel antenna and antenna module designed for efficient operation in mmWave P5G networks for connected autonomous robot applications are proposed and verified at 28 GHz. For the proposed PAAM, the beam steering has been measured at over 150°, and the 64-QAM EVM characteristics have been verified to deliver excellent performance across a wide coverage area. The extensive beam scanning angles, low side lobe levels, and minimal cross-polarization of the flat-panel structure confirm the feasibility of the proposed PAAM, which is based on a balanced multipole antenna structure

REFERENCES

[1] S. Aoki, T. Yonezawa, and N. Kawaguchi, "RobotNEST: Toward a viable testbed for IoT-enabled environments and connected and autonomous robots," *IEEE Sensors Lett.*, vol. 6, no. 2, pp. 1–4, Feb. 2022.

[2] A. Ranjha, G. Kaddoum, and K. Dev, "Facilitating URLLC in UAV-assisted relay systems with multiple-mobile robots for 6G networks: A prospective of agriculture 4.0," *IEEE Trans. Ind. Informat.*, vol. 18, no. 7, pp. 4954–4965, Jul. 2022.

[3] S. K. Jagatheesaperumal, M. Rahouti, K. Ahmad, A. Al-Fuqaha, and M. Guizani, "The duo of artificial intelligence and big data for industry 4.0: Applications, techniques, challenges, and future research directions," *IEEE Internet Things J.*, vol. 9, no. 15, pp. 12861–12885, Aug. 2022.

[4] F. Majidi, M. R. Khayyambashi, and B. Barekatain, "HFDRL: An intelligent dynamic cooperate cashing method based on hierarchical federated deep reinforcement learning in edge-enabled IoT," *IEEE Internet Things J.*, vol. 9, no. 2, pp. 1402–1413, Jan. 2022.

[5] A. Mahmood, L. Beltramelli, S. Fakhrul Abedin, S. Zeb, N. I. Mowla, S. A. Hassan, E. Sisinni, and M. Gidlund, "Industrial IoT in 5G-and-beyond networks: Vision, architecture, and design trends," *IEEE Trans. Ind. Informat.*, vol. 18, no. 6, pp. 4122–4137, Jun. 2022.
[6] B. S. Khan, S. Jangsher, A. Ahmed, and A. Al-Dweik, "URLLC and eMBB in 5G industrial IoT: A survey," *IEEE Open J. Commun. Soc.*, vol. 3, pp. 1134–1163, 2022.
[7] J. Lee, H. Lee, G.-H. Ko, D. Baek, and H. L. Lee, "Compact and highly efficient short-range radar for advanced driver assistant systems," *IEEE Trans. Veh. Technol.*, vol. 72, no. 2, pp. 1629–1637, Feb. 2023.
[8] D. Shin, W.-H. Lim, and H. L. Lee, "Highly integrated in-band full-duplex TRx antennas for mmWave V2X communications," *IEEE Trans. Veh. Technol.*, vol. 72, no. 5, pp. 6404–6411, May 2023.
[9] Y. B. Kim, J. Cho, and H. L. Lee, "MmWave self-beam-tilting antenna array with low complexity and wide coverage," *Alexandria Eng. J.*, vol. 76, pp. 323–332, Aug. 2023.
[10] W. H. Lim, S. M. Moon, and H. L. Lee, "Ka-band flat panel circularly polarized antenna array for LEO satellite communication systems," *Alexandria Eng. J.*, vol. 78, pp. 584–591, Sep. 2023.
[11] J. Park, S. Y. Lee, J. Kim, D. Park, W. Choi, and W. Hong, "An optically invisible antenna-on-display concept for millimeter-wave 5G cellular devices," *IEEE Trans. Antennas Propag.*, vol. 67, no. 5, pp. 2942–2952, May 2019.
[12] J. Park, D. Choi, and W. Hong, "Millimeter-wave phased-array antenna-in-package (AiP) using stamped metal process for enhanced heat dissipation," *IEEE Antennas Wireless Propag. Lett.*, vol. 18, no. 11, pp. 2355–2359, Nov. 2019.
[13] J. S. Chieh, E. Yeo, R. Farkouh, A. Castro, M. Kerber, R. B. Olsen, E. J. Merulla, and S. K. Sharma, "Development of flat panel active phased array antennas using 5G silicon RFICs at Ku- and Ka-bands," *IEEE Access*, vol. 8, pp. 192669–192681, 2020.
[14] S. Wang and G. M. Rebeiz, "Dual-band 28- and 39-GHz phased arrays for multistandard 5G applications," *IEEE Trans. Microw. Theory Techn.*, vol. 71, no. 1, pp. 339–349, Jan. 2023.
[15] K. Liu, S. Yang, S.-W. Qu, C. Chen, and Y. Chen, "Phased hemispherical lens antenna for 1-D wide-angle beam scanning," *IEEE Trans. Antennas Propag.*, vol. 67, no. 12, pp. 7617–7621, Dec. 2019.
[16] E. Tolin, O. Litschke, S. Bruni, and F. Vipiana, "Compact extended scan range antenna array based on Rotman lens," *IEEE Trans. Antennas Propag.*, vol. 67, no. 12, pp. 7356–7367, Dec. 2019.
[17] Z. Qu, S.-W. Qu, Z. Zhang, S. Yang, and C. H. Chan, "Wide-angle scanning lens fed by small-scale antenna array for 5G in millimeter-wave band," *IEEE Trans. Antennas Propag.*, vol. 68, no. 5, pp. 3635–3643, May 2020.
[18] X. Wang, Y. Cheng, and Y. Dong, "A wideband PCB-stacked air-filled Luneburg lens antenna for 5G millimeter-wave applications," *IEEE Antennas Wireless Propag. Lett.*, vol. 20, no. 3, pp. 327–331, Mar. 2021.
[19] B. Nie, Y. Liu, H. Lu, Z. Liu, Y. Gao, P. Zhen, and X. Lv, "Fully metallic gradient index lens array antenna for wide-angle scanning phased array," *IEEE Trans. Antennas Propag.*, vol. 71, no. 9, pp. 7363–7375, Sep. 2023.
[20] C.-M. Liu, S.-Q. Xiao, H.-L. Tu, and Z. Ding, "Wide-angle scanning low profile phased array antenna based on a novel magnetic dipole," *IEEE Trans. Antennas Propag.*, vol. 65, no. 3, pp. 1151–1162, Mar. 2017.
[21] H. Yang, X. Cao, J. Gao, H. Yang, and T. Li, "A wide-beam antenna for wide-angle scanning linear phased arrays," *IEEE Antennas Wireless Propag. Lett.*, vol. 19, no. 12, pp. 2122–2126, Dec. 2020.
[22] W.-H. Zhang, Q. Xue, S. Liao, W. Che, and W. Yang, "Low-profile compact microstrip magnetic dipole antenna with large beamwidth and broad bandwidth for vehicular applications," *IEEE Trans. Veh. Technol.*, vol. 70, no. 6, pp. 5445–5456, Jun. 2021.
[23] H. Cho, H.-W. Jo, J.-W. Kim, K.-S. Kim, J.-I. Oh, and J.-W. Yu, "Shorted trapezoidal SIW antenna with quasi-hemispherical pattern for 2D wide scanning planar phased array antenna," *IEEE Trans. Antennas Propag.*, vol. 70, no. 8, pp. 7211–7216, Aug. 2022.
[24] Y.-B. Kim, H.-J. Dong, K.-S. Kim, and H. L. Lee, "Compact planar multipole antenna for scalable wide beamwidth and bandwidth characteristics," *IEEE Trans. Antennas Propag.*, vol. 68, no. 5, pp. 3433–3442, May 2020.
[25] Y.-B. Kim, S. Lim, and H. L. Lee, "Electrically conformal antenna array with planar multipole structure for 2-D wide angle beam steering," *IEEE Access*, vol. 8, pp. 157261–157269, 2020.



YE-BON KIM received the B.S. and M.S. degrees in electrical and electronics engineering from Chung-Ang University, Seoul, South Korea, in 2018 and 2020, respectively, where he is currently pursuing the Ph.D. degree. His research interests include smart antenna, phased array antennas, mmWave antennas, antenna-in-package, RF circuit, and antenna calibration.



JONG-SIK MIN received the B.S. degree from Chung-Ang University, Seoul, South Korea, in 2022, where he is currently pursuing the M.S. degree in intelligent semiconductor engineering. His research interests include mmWave antenna design, phased array antennas, and heat dissipation antennas.



SEONG-MO MOON received the B.S., M.S., and Ph.D. degrees in electrical engineering from the University of Seoul, Seoul, South Korea, in 2003, 2005, and 2010, respectively. From 2005 to 2008, he was a Senior Research Engineer at Analog Devices Inc., Seongnam, South Korea, where he was involved in RFIC design such as voltage controlled oscillator (VCO) and local oscillator (LO) generation blocks. He is currently working as a Senior Engineer with the Electronics and Telecommunications Research Institute (ETRI), Daejeon, South Korea. He is currently involved in the development of RF and Digital modules and systems for next generation satellite payload. His research interests include design and analysis of microwave and mmWave active components such as beamforming IC, power amplifier, and oscillator, and design of RFICs and MMICs based on silicon, gallium arsenide (GaAs), and gallium nitride (GaN) for satellite payloads.



HAN LIM LEE (Member, IEEE) received the B.A.Sc. degree in electronics engineering from Simon Fraser University, BC, Canada, in 2008, and the M.S. and Ph.D. degrees in electrical engineering from KAIST, Daejeon, South Korea, in 2010 and 2014, respectively. From 2014 to 2015, he was a Senior Engineer at the DMC Research Center, Samsung Electronics. In 2015, he joined the School of Electrical and Electronics Engineering, Chung-Ang University, where he is currently working as an Associate Professor. His research interests include microwave/RF circuits and communication systems, mmWave beamforming antennas and phased array systems, antenna-in-package (AiP), RFIC/MMIC, thermally effective RF design, microwave wireless power transmission (MWPT), RF energy harvesting, and sensor embedded smart antenna systems.